BNL-63358

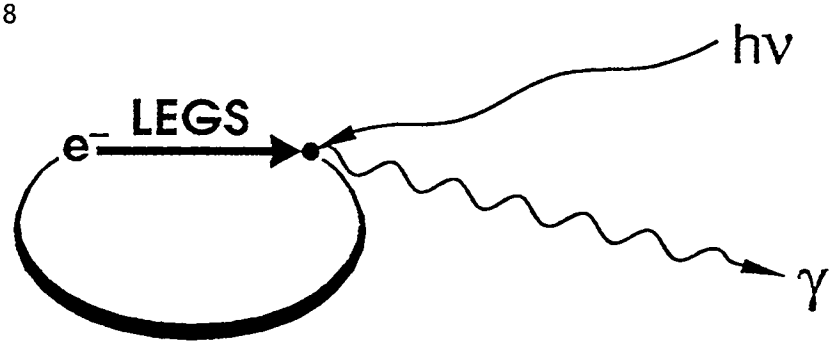

Laser Electron Gamma Source

Biennial Progress Report - June, 1996

(A.M. Sandorfi, *editor*)

LASER ELECTRON GAMMA SOURCE

BROOKHAVEN NATIONAL LABORATORY
ASSOCIATED UNIVERSITIES, INC.
Under Contract No. DE-AC02-76CH00016 with the
UNITED STATES DEPARTMENT OF ENERGY

DISCLAIMER

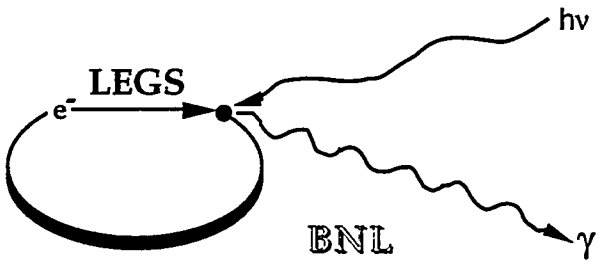

Laser Electron Gamma Source†

Brookhaven National Laboratory

Biennial Progress Report - June, 1996
(A.M. Sandorfi, *editor*)

LEGS Facility Overview

A. Caracappa[1], S. Hoblit[1], O.C. Kistner[1], A. Kuczewski[1], F. Lincoln[1], M. Lowry[1], M. Lucas[2], L. Miceli[1], A.M. Sandorfi[1], C.E. Thorn[1], and J. Tonnison[3]

[1]Physics Department, Brookhaven National Laboratory, Upton NY 11973
[2]Department of Physics, University of South Carolina, Columbia SC 29208
[3]Department of Physics, Virginia Polytechnic Institute & SU, Blacksburg, VA 24061

The LEGS facility provides intense, polarized, monochromatic γ-ray beams by Compton backscattering laser light from relativistic electrons circulating in the X-Ray storage ring of the National Synchrotron Light Source at Brookhaven National Laboratory. Since 1990, experiments have concentrated on single polarization observables (polarized beams on unpolarized targets) in nuclear reactions involving the Δ resonance. Highlights of the last two years is given below. An updated status of LEGS, and recent publications, is available on the WWW via http://WWW.LEGS.BNL.GOV/~LEGS/.

In 1997 a new phase of operations will begin, focusing on double-polarization measurements with circularly polarized photon beams and longitudinally polarized nucleon targets. This work requires the development of (i) a new frozen-spin hydrogen-deuteride target that provides high polarizations for both nuclear species, and (ii) a new large acceptance detector array for measuring total reaction cross sections in both neutral and charged-particle channels. Progress on these instrumentation developments is an ongoing effort of the LEGS Spin Collaboration (LSC) and is discussed in the last section of this report.

† Supported by the US Department of Energy under contract # DE-AC02-76CH00016.

Spin Asymmetries from $^{16}O(\vec{\gamma},p\pi^-)$ near Δ Resonance Energies (Exp. L 13)

K. Hicks[2], H. Baghaei[5], A. Caracappa[1], A. Cichocki[5], G. Davenport[2], R. Finlay[2], V. Gladyshev[5], T. Gresko[5], S. Hoblit[1], M. Khandaker[6], O. Kistner[1], A. Kuczewski[1], F.X. Lee[4], R. Lindgren[5], M. Lucas[3], L. Miceli[1], B. Norum[5], J. Rapaport[2], A. Sandorfi[1], R. Sealock[5], L.C. Smith[5], C. Thorn[1], S. Thornton[5], C.S. Whisnant[3], and L.E. Wright[2]

[1]Physics Department, Brookhaven National Laboratory, Upton N.Y.,11973;
[2]Department of Physics, Ohio University, Athens, OH 45701
[3]Department of Physics, University of South Carolina, Columbia S.C.,29208;
[4]TRIUMF, 4004 Wesbrook Mall, Vancouver, B.C., V6T 2A3, Canada;
[5]Department of Physics, University of Virginia, Charlottesville Va.,22903;
[6]Physics Department, Virginia Polytechnic Institute & SU, Blacksburg Va.,24061.

Pion photoproduction from hydrogen and deuterium targets has been used to determine the vertex couplings $g_{\gamma N\Delta}$ which measure the transition strength for Δ resonance [1]. When the nucleon is embedded in the nucleus, the vertex terms will be "dressed" by off-shell effects. In addition, the nuclear medium is expected to interact with the Δ resonance, resulting in a Δ-nucleus potential and new decay channels (such as ΔN→NN for example). The description of these medium effects is of considerable interest. For example, the ratio between quasifree π^+ -p and quasifree π^- -p scattering with nuclear targets is substantially modified from the ratio for a proton target [2], showing strong evidence for a modified Δ in the nuclear medium. Pion photoproduction provides a means to investigate medium modifications of the Δ in a theoretical model that has fewer ambiguities than for models of pion scattering.

Although theoretical models for *inclusive* pion photoproduction have enjoyed some success at lower energies, at Δ resonance energies the calculations predict cross sections which are much lower than the data. In order to investigate the reason for this, we turn to exclusive reactions. Exclusive pion photoproduction allows the struck nucleon to leave the nucleus, which largely removes the sensitivity to the nuclear structure of the target observed in the inclusive A (γ,π)A reaction. A particular advantage is gained by measuring the spin asymmetry, $\Sigma = (\sigma_{\parallel} - \sigma_{\perp}) / (\sigma_{\parallel} + \sigma_{\perp})$, which is insensitive to the choice of optical potential or the spectroscopic factor used in the calculations [3]. The calculations for Σ are, however, sensitive to the parameters of the Δ propagator [3], which carries information on the Δ-nucleus potential.

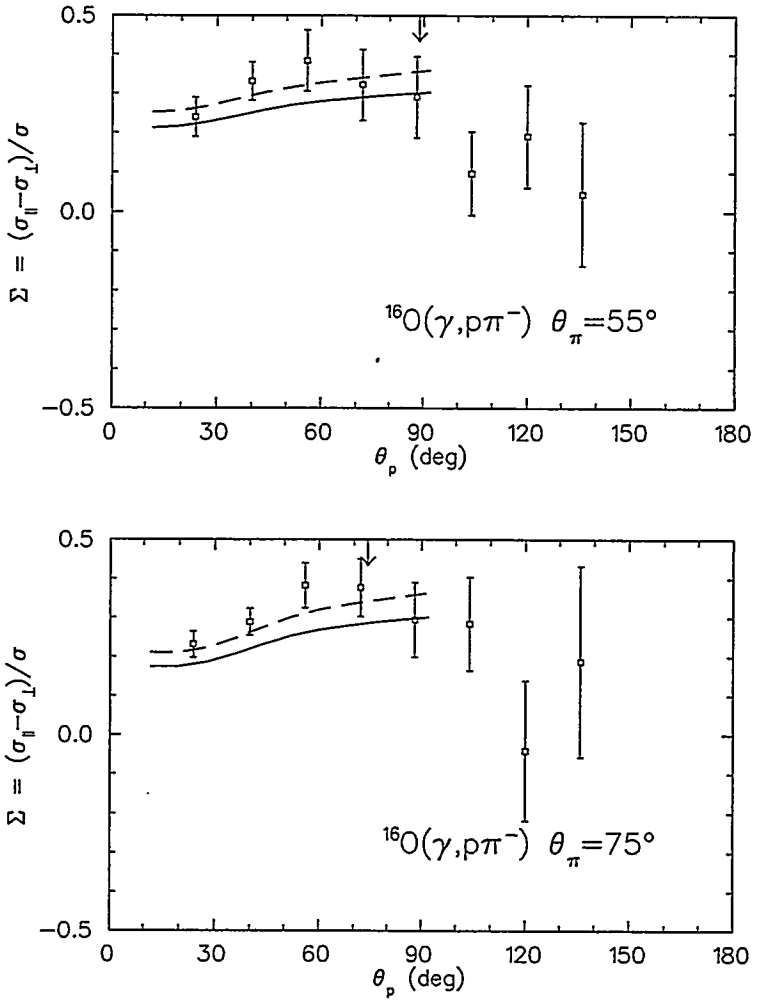

Fig.1. Spin asymmetries at 293 MeV for the photon polarization in and normal to the reaction plane, for the pion angles shown, as a function of proton angle (lab). The curves represent PWIA calculations with the Δ mass at its free value (solid) and reduced by 5% (dashed).

Cross sections for the exclusive $^{12}C(\gamma,\pi^-p)$ reaction have been reported in the literature [4]. Although these data have large statistical uncertainties, the theoretical model, which assumes no modification to the Δ propagator, overpredicts these data by a factor of more than 3 at forward pion angles. At backward angles, where the Δ contribution is smaller, the disagreement is less severe. If the effective mass in the Δ propagator is reduced by an amount between 5% and 10% in the model, as an approximation to inclusion of a Δ-nucleus potential, then better agreement with the data is obtained. This effect can now be compared to new measurements of the spin asymmetry.

Asymmetries for the $^{16}O(\gamma,p\pi^-)$ experiment are shown in Fig. 1 at two pion reaction angles, as a function of the accompaning proton angle, for 293 MeV incident beam. Both data and calculations have been averaged over all proton and pion energies at the given angles, with a threshold energy such that the outgoing particles escape the target volume and trigger the scintillators. The momentum transfer to the residual nucleus, q, is largely determined by the proton angle. For reference, the location of q =200 MeV/c is plotted in the figure for each pion angle as an arrow along the top scale. The harmonic oscillator wave functions used in the calculations are not expected to be valid much outside this ~1 fm^{-1}.

Also plotted in the figure are theoretical curves where the mass of the Δ is unmodified (solid line), or has been reduced by 5% (dashed line). The latter models an attractive Δ-nucleus potential, with a ~ 50 MeV well depth. Of course, this can only be used as an indication of whether the calculations are sensitive to this potential, and not to set rigid limits on the range of the potential depth, which requires a more sophisticated dynamical model. Nonetheless, the data do show better agreement with the modified Δ mass curves, suggesting that further calculations and more precise data would be useful. Comparison of these model predictions with the unpolarized cross sections are also potentially informative, and these are under analysis.

[1] K.I. Blomqvist and J.M. Laget, Nucl. Phys. **A280**, 405(1977).
[2] G.S. Kyle, *etal*, Phys. Rev. Lett. **52**, 974 (1984).
[3] X. Li, L.E. Wright and C. Bennhold, Phys. Rev. **C48**, 816 (1993).
[4] L.D. Pham, *et al.*, Phys. Rev. **C46**, 621 (1992).

Deuteron PhotoDisintegration and coupled NΔ/NN interaactions (Exps. L1,3)

The LEGS Collaboration:

G. Blanpied[4], M. Blecher[6], A. Caracappa[1], C. Djalali[4], M-A. Duval[4], G. Giordano[2], K. Hicks[8], S. Hoblit[5], M. Khandaker[1,6], O.C. Kistner[1], G. Matone[2], L. Miceli[1], W.K. Mize[4], B.M.Preedom[4], D. Rebreyend[4,9], A.M.Sandorfi[1], C. Schaerf[3], R.M. Sealock[5], C.E. Thorn[1], S.T.Thornton[5], K. Vaziri[7], C.S. Whisnant[1,4] and X. Zhao[6] and P. Wilhelm[10] and H. Arenhövel[10]

[1] Physics Department, Brookhaven National Laboratory, Upton N.Y., 11973
[2] INFN-Laboratori Nazionali di Frascati, Frascati Italy
[3] Università di Roma "Tor Vergata" and INFN-Sezione di Roma2, Rome Italy
[4] Department of Physics, University of South Carolina, Columbia S.C., 29208
[5] Department of Physics, University of Virginia, Charlottesville Va., 22903
[6] Physics Department, Virginia Polytechnic Institute & SU, Blacksburg Va., 24061
[7] Rensselaer Polytechnic Institute, Troy, N.Y., 12180-3590
[8] Department of Physics, Ohio University, Athens, OH, 45701
[9] Institut des Science Nucleaires, IN2P3-UJF, 38026 Grenoble cedex, France
[10] Institut für Kernphysik, Johannes Gutenberg-Universität, D-55099 Mainz, Germany

Five independent measurements of the $d(\vec{\gamma},p)n$ reaction have been carried out at LEGS (Exps. L1 and L3) with three different detector systems, different photon end-points from different laser wavelengths, different polarizations and two different liquid deuterium targets. These measurements overlap in various kinematic regions between 113 and 325 MeV, and the agreement in the regions of overlap is excellent. By taking weighted means of overlapping measurements, a 'net' data base has been constructed, and is available from the LEGS WWW page[1]. Selections of these results have recently appeared in ref. [2] where comparisons are made to recent coupled-channel calculations. These are in agreement with cross sections measured with linear polarization parallel to the reaction plane but fail to

account for data taken with perpendicular kinematics, as shown in the 300 MeV data to the right. (Note the suppressed zero.) The shaded band reflects uncertainties in π-MEC components.

At present, there is no clear explanation for the success of the coupled-channel calculations in one polarization kinematics and their failure for the orthogonal state. Spin observables provide a considerably more sensitive test of the angular momentum modeling than cross sections. Although the model parameters of the calculations discussed here were fitted to NN phase shifts, all assumed static NN potentials, with retardation effects included only in the NΔ and NN-NΔ-transition potentials. The additional use of retarded potentials in the NN interaction could significantly alter the angular momentum decomposition.

[1] LEGS Data Release #**L1-3.0**, March/94, available via http://WWW.LEGS.BNL.GOV/~LEGS/ .
[2] LEGS Collaboration, G.S. Blanpied et al., Phys. Rev. C **52**, R455 (1995).

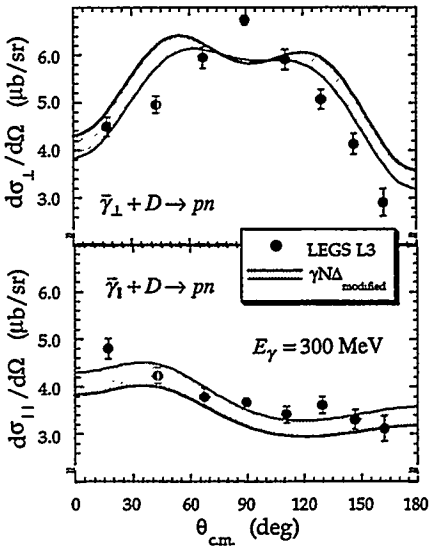

Fig.1. Angular distributions at 300±5 MeV.

First Multipole Analysis of $D(\vec{\gamma},p)n$

C.S. Whisnant[2], A.M.Sandorfi[1] and D. Pomarede[2,1]

[1]Physics Department, Brookhaven National Laboratory, Upton N.Y., 11973
[2]Department of Physics, University of South Carolina, Columbia S.C., 29208

To investigate the origins of discrepancies between the LEGS D(γ,p)n data and the recent coupled-channel calculations, an energy dependent multipole analysis of the complete data set is in progress.

The multipole expansion includes electric and magnetic dipole and quadrupole couplings in the initial state and relative p-n angular momenta up to l=4 in the final state. This gives the cross section and beam asymmetry in terms of 22 complex multipoles. These are written as a magnitude and a phase, with the latter assumed to be given by Watson's theorem. Even through the data extends to energies above the two pion threshold, deviations from this assumed energy dependence are expected to be small and are absorbed into the energy dependence of the magnitudes. This assumption leaves 22 free parameters. Each of these are in turn parameterized with up to a quadratic energy dependence, raising the maximum number of parameters to 88. Obviously, with such a large number of free parameters some guidance is required to select a meaningful subset and a procedure to

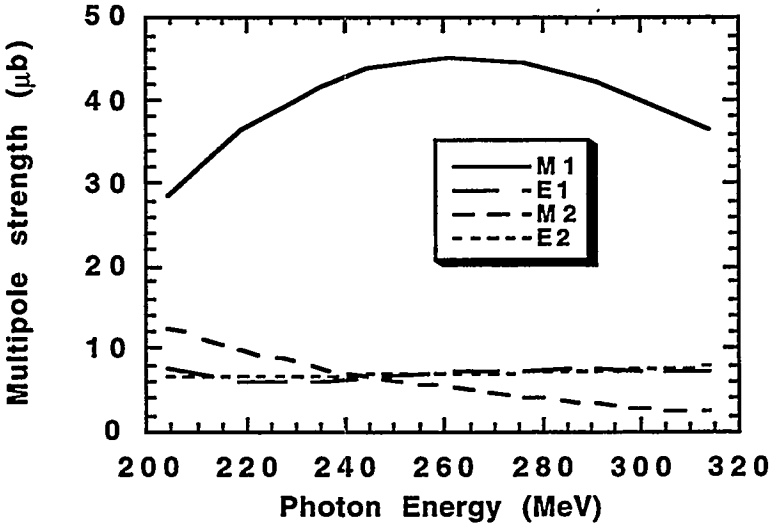

Fig. 1. Multipole strengths resulting from the analysis described above. The sum of these multipole strengths gives the total cross section.

adjust them. This guidance is found by inspecting the multipoles predicted by coupled channel calculations of P. Wilhelm and H. Arenhövel (private communication). Here we find that, roughly speaking, the large relative angular momenta in the final state tend to dominate and, as expected, M1 photon coupling is strongest.

Guided by these observations, fits were made to the data using the CERN minimization package *MINUIT*. There are 11 energies, each with 8 cross section sums [$d\sigma/d\Omega = 1/2(d\sigma_{\parallel}/d\Omega + d\sigma_{\perp}/d\Omega)$] and differences [$\Delta = 1/2\ (d\sigma_{\parallel}/d\Omega - d\sigma_{\perp}/d\Omega)$], as well as the integrated total cross section, giving 187 data points. Beginning with the dominant terms as described above, successive fits were made, adding parameters until the reduced chi-square, χ^2/N_{free}, showed no significant improvement as determined by the F-test. At this point, all parameters for which their uncertainty equaled or exceeded their values were set to zero and the fit was repeated one last time. This procedure results in an 18 parameter fit with $\chi^2/N_{free} = 1.88$. The total multipole strengths are shown in figure 1.

As expected, the M1 multipole dominates the cross section. It is described by a quadratic energy dependence in the $^1D_2$ and a smaller, constant, $^1S_0$ contribution. The M2 contribution is given solely by the $^3F_3$ term. The E1 photon coupling is given by $^3P_0$, $^3P_1$ and $^3F_2$ contributions and the E2 by $^3D_1$, $^1D_2$, $^3D_3$, and $^3G_3$ terms. Typical of the agreement between the data and the fit are the angular distributions at 300 MeV shown in figure 2. Fitting all angles and energies at once produces a smooth fit that represents an average of the entire data set. A simple estimate of the uncertainty in this average is obtained from the standard deviation of the distribution of the difference between the data and the fit for the sum and difference cross sections. In figure 3, we see that this distribution is symmetric with a FWHM of 0.40 μb/sr, corresponding to a standard deviation of 0.18 μb/sr. From this we estimate the uncertainty in the fitted cross sections $\delta = \sigma/\sqrt{N} = (0.18\ \mu b/sr)/\sqrt{176} = 0.013\ \mu b/sr$. The energy and angle dependence of this uncertainty as well as the uncertainties in the multipole moments themselves are obtained from the complete covariance matrix. A detailed investigation is in progress. First estimates yield uncertainties the same order of magnitude as the simple estimate above. The multipole moments have uncertainties ranging from about 5% for the larger components to almost 50% for the smallest.

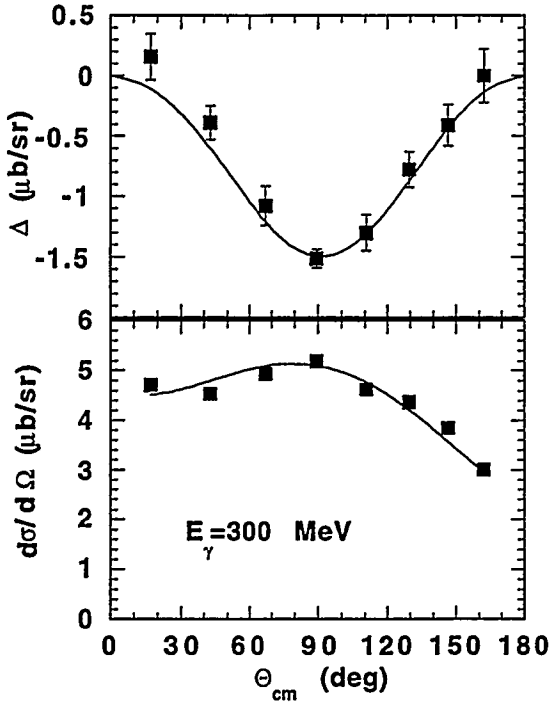

Fig. 2. The energy and angle dependent fit compared to the cross section sum and polarization difference at 300 MeV. The uncertainties on the cross section sum data are smaller than the plotting symbol.

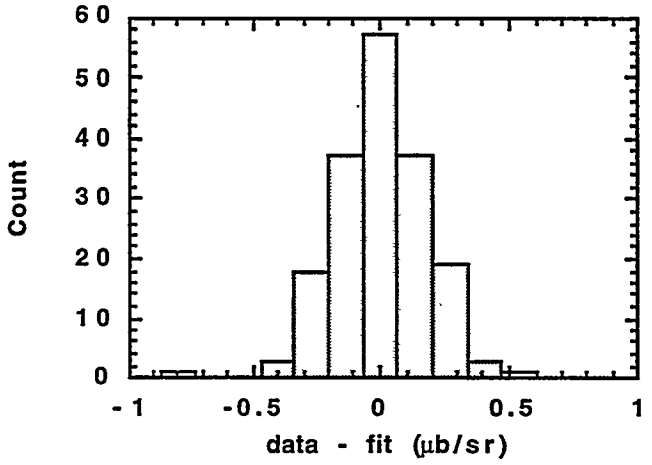

Fig. 3. A histogram of the difference between the data and the fit for the sum and difference cross sections.

The E2 $N \rightarrow \Delta$ Transition from $p(\vec{\gamma},\pi)$ and Compton Scattering (Exps. L7,8)

The LEGS collaboration

G. Blanpied[4], M. Blecher[6], A. Caracappa[1], C. Djalali[4], G. Giordano[2], K. Hicks[7], S. Hoblit[5,1], M.A. Khandaker[6,1], O.C. Kistner[1], M. Lucas[4], G. Matone[2], L. Miceli[1], B.M.Preedom[4], D. Rebreyend[4], A.M.Sandorfi[1], C. Schaerf[3], R.M. Sealock[5], H. Ströher[8], C.E. Thorn[1], S.T.Thornton[5], J. Tonnison[6], C.S. Whisnant[4], H. Zhang[7] and X. Zhao[6]

[1]Physics Department, Brookhaven National Laboratory, Upton N.Y.,11973;
[2]INFN-Laboratori Nazionali di Frascati, Frascati Italy;
[3]Universita di Roma and INFN-Sezione di Roma,Rome Italy;
[4]Department of Physics, University of South Carolina, Columbia S.C.,29208;
[5]Department of Physics, University of Virginia, Charlottesville Va.,22903;
[6]Physics Department, Virginia Polytechnic Institute & SU, Blacksburg Va.,24061.
[7]Department of Physics, Ohio University, Athens, OH 45701
[8]II Physikalisches Institut, Universitat Gießen, Germany

In constituent quark models, a tensor interaction, mixing quark spins with their relative motion, is introduced to reproduce the observed baryon spectrum. This necessarily results in a D-wave component in the nucleon wave function, which breaks spherical symmetry and leads to a static deformation for the proton's first excited state, the Δ resonance. The Δ is photo-excited mainly by M1 radiation. However, the D-state component results in a small E2 transition strength. The magnitude and sign of the E2/M1 mixing ratio are quite sensitive to the internal structure of the proton.

The isospin I=3/2 Δ decays with a 99.4% branch to πN final states, and with an 0.6% γN branch back to the initial state (Compton scattering). (Of the π channels, (γ,π^+) is the least sensitive due to large Born contributions coming from the t-channel.) Isolating the N$\rightarrow\Delta$ transition requires a decomposition of the multipoles into resonant and background components. This decomposition requires a model, and model dependences enter the analysis of π-production and Compton scattering in different ways. These two branches have different E2 sensitivities and both have been studied at LEGS.

The $p(\vec{\gamma},\pi^o)$ and $p(\vec{\gamma},\gamma)$ reactions were separated by detecting photons in a high resolution NaI(Tl) spectrometer, together with the recoil protons whose trajectories were tracked through wire (drift) chambers and whose energies were measured, both by energy deposition and by time of flight in an array of plastic scintillators. This arrangement is shown in figure 1. The full data set consisted of 3 sets of runs with different NaI and scintillator-bar orientations, chosen to provide overlap angles. The π^o/Compton separation for the full data set centered at 90° c.m. is shown in figure 2 where the γ-ray energy is plotted against the recoil proton energy. Here, the γ and recoil energies for Compton scattering, as calculated from the tagged beam energy and the proton recoil angles measured in the drift chambers, have been subtracted. Compton scattering is clearly resolved here, and in *all* other runs.

In $p(\gamma,\pi)$, the observable most sensitive to an E2 component is the cross section, $\sigma_{\parallel}$, for π^o production by linearly polarized photons whose electric vector is oriented parallel to the reaction plane [1].

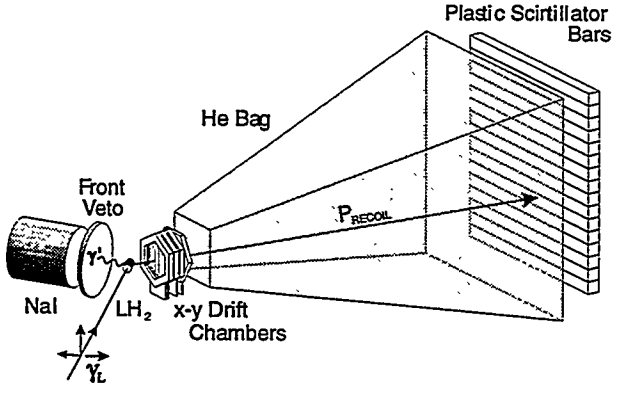

Fig.1. The detector arrangement used to separate the (γ,π) and (γ,γ) reactions (see text).

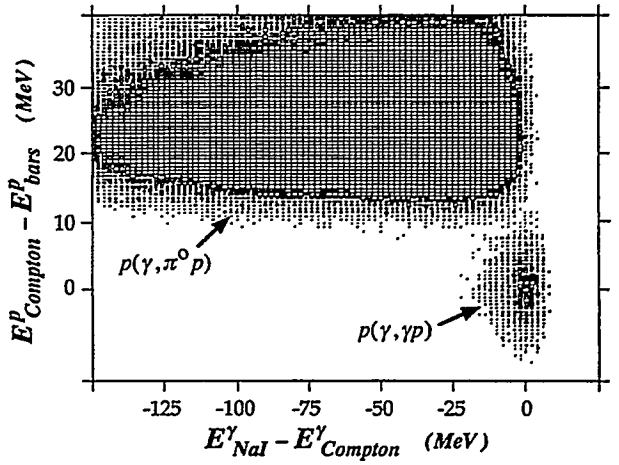

Fig. 2. The π^o/Compton separation with the detectors of fig. 1.

The corresponding cross section for the perpendicular orientation, $\sigma_\perp$, is completely insensitive to E2 excitation at all but extreme angles. Thus, the ratio $\sigma_\parallel/\sigma_\perp$ maximizes E2 sensitivity, while dividing out systematic uncertainties. The first new measurements of this ratio over a limited angular range suggested E2 transition strengths significantly larger than expected from previous multipole analyses [1-3]. In our 1994 LEGS Progress Report [4], and at the SPIN'94 Conference [5], we presented the results of new measurements of this π^0 polarization ratio taken over a large angular range, and these were compared to the model predictions of Davidson, Mukhopadhyay and Wittman (DMW) [6]. This model contains five free parameters, G_E and G_M, the electric and magnetic coupling constants at the $\gamma N\Delta$ vertex, and three constants parameterizing the off-shell behavior. In addition to the polarization ratios, cross sections are needed to fix these 5 parameters. Since absolute cross sections from our experiments were not available at the time, our polarization data was combined with previously published unpolarized results from other laboratories. The results of fitting this composite data set to the DMW parameters gave a value for $-G_E/G_M$ (the $N\rightarrow\Delta$ part of the E2/M1 mixing ratio) of **$-2.7\pm0.1\%$** [4,5]. (The error of $\pm0.1\%$ reflected only the variations in the methods of unitarizing the pion amlitudes.)

The analysis of the LEGS experiments are now complete. We present here a selection of cross section and polarization data for both Compton scattering and π-production, and examine the consistency of previous E2/M1 determinations in the light of the full data set. The 90° excitation functions for the two reactions are shown below in figures 3 and 4.

There had been a long standing discrepancy between earlier Compton measurements and dispersion calculations that used π-production as input. The LEGS measurement was designed to remove all of the uncertainties associated with separating Compton scattering from the π^0 channel by a large overdetermination of kinematic parameters. Both reactions are completely specified by two kinematic observables. In this experiment, six quantities were measured, the beam energy, the scattered γ-ray energy, the polar and azimuthal angles of the recoil proton, and the proton's TOF and energy. This large degree of over-determination has two important consequences. First, it guarantees an accurate separation of the two competing channels (figure 2). Secondly, it enables all detector efficiencies to be

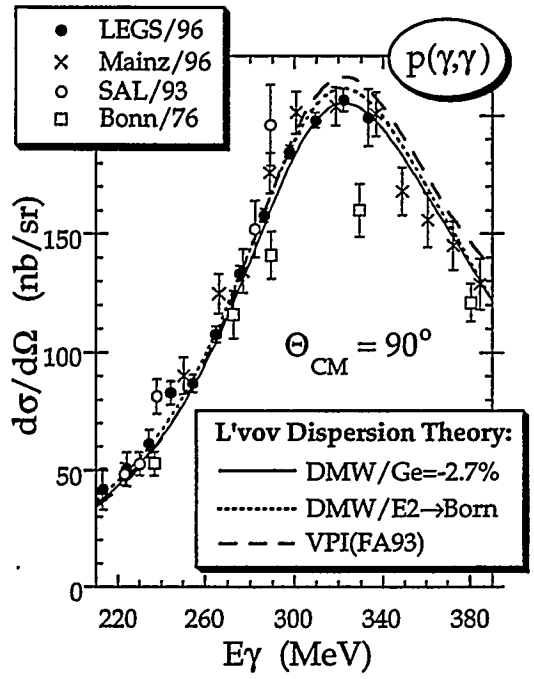

Fig.3. The LEGS Compton scattering cross sections at 90° (solid pts.) [7], compared with recent data from Mainz [8] and SAL [9], and earlier data from Bonn [10]. In addition to the indicated errors errors, the systematic scale uncertainties are ~2% (LEGS), 5% (Mainz), 3.9% (SAL), and 4.4% (Bonn).

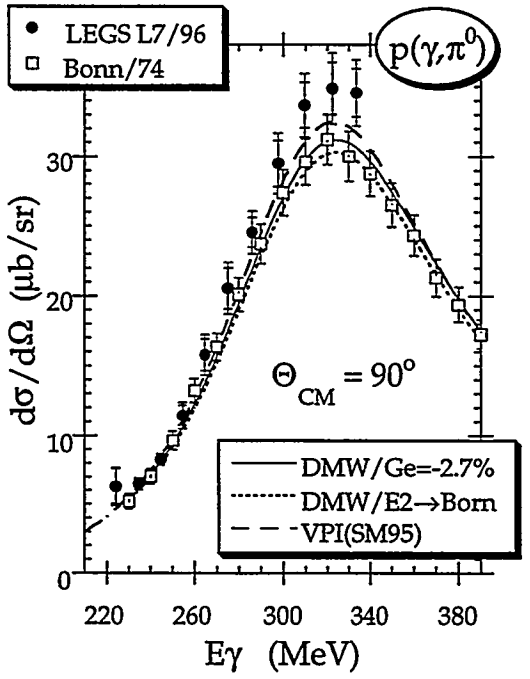

Fig.4. The LEGS π^0 cross sections at 90° (solid pts.) compared with earlier data from Bonn [11]. Two error bars are shown for each point, the smaller reflects the measurement error (statistical, and other sampled uncertainties) and the larger includes systematic scale errors added linearly (see text).

evaluated directly from the data itself, without resorting to simulations and thus avoiding their associated uncertainties. For the Compton events, the geometric solid angle was entirely determined by the recoil proton detectors. This, and the effect of the finite target length, were modeled by Monte Carlo simulations and different angular acceptances, determined by the wire chambers, produced consistent results. The data shown as solid points in figure 3 reflect all statistical and *polarization-dependent* systematic errors [7]. Additional systematic scale errors are less than 2%. Near the peak of the Δ, our results are substantially higher than the earlier measurements (open squares [10], for example). Other recently published measurements from Mainz [8] (crosses) and from SAL [9] (circles) are in excellent agreement. Data from earlier experiments at Cornell (1961), Tokyo (1964), Illinois (1967), and Bonn (1976) at energies higher or lower than the Δ peak are either consistent or slightly lower than these new measurements [see refs. in 7]. Why the earlier results are so dramatically lower near the resonance energy is not known.

For the π^o channel, yields and detector efficiencies were likewise determined directly from the same data sets as Compton scattering. However, the geometrical acceptance was necessarily a convolution of the proton recoil and γ-ray arms, rather than being simply defined by only one. For these analysis, cuts were set to exclude any regions where the measured detector efficiencies were rapidly varying. This corresponds to a relatively large acceptance. The results from any further cuts then expose the uncertainty in the geometrical acceptance. Successive cuts were imposed to explore such variations, down to the limit where all photons are in fact confined to a radius less than the NaI collimator, which completely removes the NaI arm from the solid angle. (This restrictive "*Compton-like*" cut passes only those γ-rays above a high energy threshold and essentially transferes the uncertainty to the response function of the NaI.) Between 8 and 12 different analysis conditions were used to determine each data point. (Generally, the cuts restrict the energy and angle acceptance so that the number of contributing analyses varies from point to point.) The net cross sections were computed as the mean of these values. The standard deviation of these results was used as the sampled measure of the uncertainty in the geometrical acceptance. This was combined in quadrature with the statistical error of the full set with minimal cuts (typically 1%) to yield a net measurement error. This is shown as the smaller of the two bars on the solid points of figure 4. To this, the combined systematic flux normalization and target thickness scale uncertainty of 1.9% was added linearly. This total resulting uncertainty is plotted as the larger of the two error bars in figure 4. For comparison, the 1974 Bonn data are also shown. In the Bonn analysis, the *measurement errors* are purely statistical and are generally smaller than the symbols, while estimates for the uncertainty in detector acceptance were included as part of the larger systematic errors. The π^o results show a generally similar trend to Compton scattering when compared to the Bonn data, namely agreement at lower energies but higher cross sections near the Δ peak. For π^o-production the full errors just touch while for Compton scattering the disagreement is larger. This result is admittedly surprising in light of new π^o data from Mainz that are much closer to the old Bonn results [12]. (The Mainz π^o experiments were different measurements, not simultaneous with those that produced the crosses in figure 3.)

Angular distributions of the cross sections and linear polarization observables, near the Δ peak, for Compton scattering and π^o-production are shown as the solid points in figures 5 and 6. The recent Mainz 90° Compton cross section is plotted in the top panel of figure 5. For the Compton asymmetry, the only previously published datum (from Frascati) is also shown. For π^o production, the results of applying the most restrictive cuts to the LEGS data ("*Compton-like*" kinematics), are shown with statistical errors as the crosses at 90° and 120° in the top panel of figure 6. Also plotted are the older Bonn and Lund cross sections, and a Khar'kov asymmetry measurement, from refs. [11,14,15].

Three sets of curves for $p(\gamma,\pi^o)$ are plotted in figures 4 and 6. The solid curves are the calculations described in refs. [4,5] in which the parameters of the DMW model were optimized to reproduce a combination of the LEGS π^o polarization ratio results, together with the Bonn unpolarized cross sections from ref. [11]. This was the exercise carried out with the first new results that yielded the value of –2.7 % for $-G_E / G_M$. The result of turning off the E2 part of the N→Δ transition in this calculation (G_e=0) is shown as the dotted curve. (Setting the entire E2 amplitude, including Born contributions, to zero produces dramatic effects but is not terribly informative.) For comparison, the predictions of current VPI multipole analyses are shown as the dashed curves [16]. Although the DMW and VPI predictions are both quite close to the π^o polarization data, the cross section predictions indicate a need for some readjustment of parameters.

Compton scattering provides an additional constraint on this problem. The imaginary parts of the Compton amplitudes can be calculated from (γ,π) multipoles using s- and u-channel unitarity, and dispersion integrals can be written for their real parts. Four of these integrals converge rapidly with energy. However the remaining two, those involving a photon helicity flip, do not converge rapidly, making subtractions essential. One of these is dominated by t-channel π^0 exchange, the *Low* amplitude, and can be readily evaluated in terms of the π^0 lifetime. However, the other contains contributions from multiple meson exchange in the t-channel that are quite poorly determined. However, L'vov has developed a model in which sum rules are used to write the subtraction function for this spin-flip amplitude in terms of the difference of the proton polarizabilities [17], which can then be fixed by fitting a perturbative expansion of the cross section to data below π-threshold. The solid, dotted, and dashed

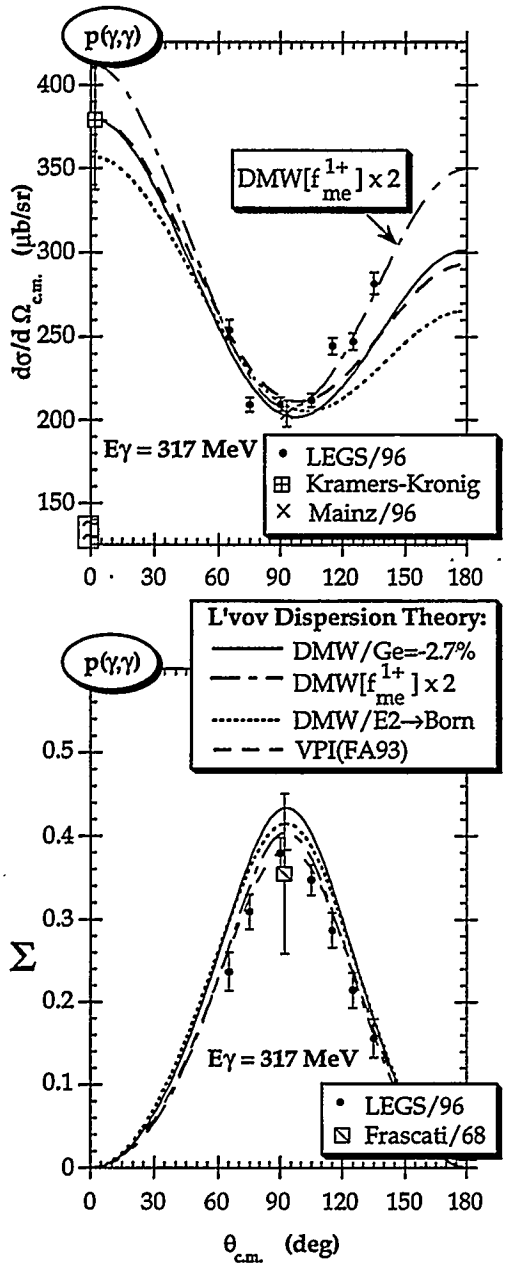

Fig.5. Angular distributions for the unpolarized cross section and linear polarization asymmetry in p(γ,γ) from LEGS (solid circles). Other data are from refs. [8, 13].

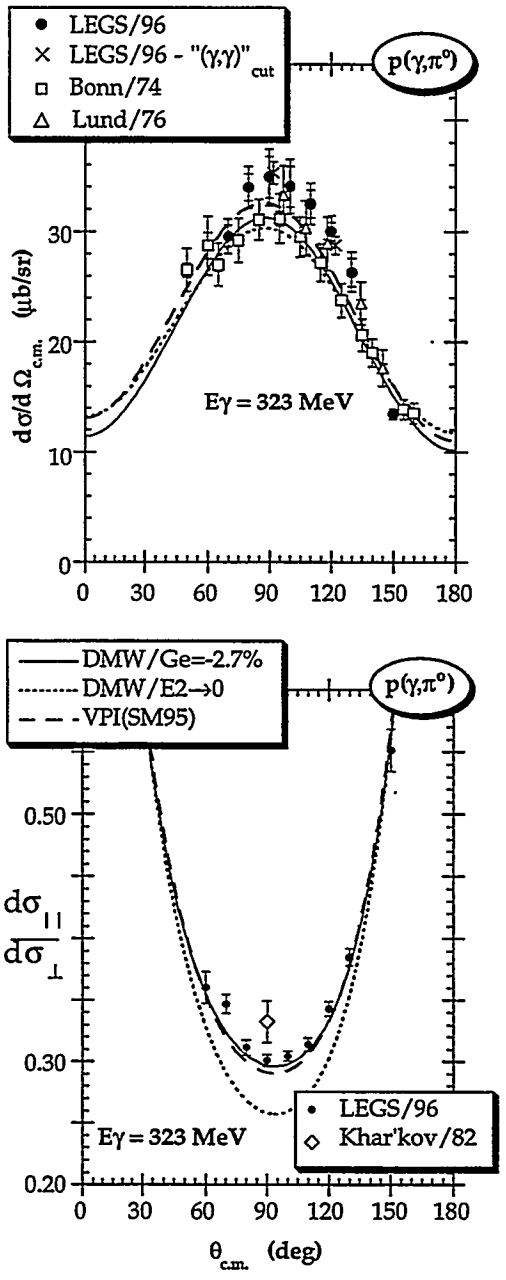

Fig.6. Angular distributions for the unpolarized cross section (top) and polarization ratio (bottom) in p(γ,π^0) from LEGS (solid circles). Other data are from refs. [11, 14, 15].

curves in figures 3 and 5 have been calculated in this way using as input the pion multipoles corresponding to the three calculations in figures 4 and 6. In particular, the predictions of the solid and dashed curves started with the DMW model (adjusted to give G_e=-2.7% of G_m) and with recent VPI multipole analyses of π-production, while the dotted curves were obtained by setting the $E2^{j=3/2}$ Compton multipoles to their s- and u-channel Born and t-channel pole values.

The Compton cross sections at back angles are quite sensitive to E2/M1 interference and these *are not reproduced* by either the solid or dashed curves. The prediction corresponding to the solid curve also gives the poorest description of the polarization asymmetry. The leading E2 interference term, f^{l+}_{me} corresponding to E2 photoexcitation followed by M1 decay, is dominated by the N→Δ transition [18]. Doubling this amplitude results in the long-dashed/short-dashed curves in figure 5, which seem to describe most of the cross section data, although the asymmetry remains a little high.

The new Compton results clearly show the deficiencies in our earlier estimate of $-G_E / G_M$=–2.7% which was driven solely by the pion polarization data. They in fact suggest an E2/M1 value that is considerable larger. A complete determination of the E2 component in N→Δ requires a simultaneous fit to both Compton scattering and π-production. This is presently under way.

[1] LEGS Collaboration, G.S. Blanpied *et al.*, Phys. Rev. Lett. **69**, 1880 (1992).
[2] R. Davidson and N. Mukhopadhyay, Phys. Rev. Lett. **70**, 3834 (1993).
[3] A.M. Sandorfi and M. Khandaker, Phys. Rev. Lett. **70**, 3835(1993).
[4] LEGS Biennial Progress Report, June 1994 (ed. A.M. Sandorfi), BNL-**60698** (1994).
[5] A.M. Sandorfi, Int. Sym. High Energy Spin Physics and Polarization Phenomena in Nuclear Physics, Bloomington, IN, 1994 (edited by E.J. Stephenson and S. Vigdor), AIP Conf. Proc. No. **330** (AIP, Woodbury, NY, 1995), p.230.
[6] R. Davidson, N. Mukhopadhyay and R. Wittman, Phys. Rev. **D43**, 71 (1991).
[7] LEGS Collaboration, G.S. Blanpied *et al.*, Phys. Rev. Lett. **76**, 1023 (1996).
[8] C. Molinari *et al.*, Phys. Lett. **B371**, 181 (1996).
[9] E.L. Hallin *et al.*, Phys. Rev. **C48**, 1497 (1993).
[10] H. Genzel *et al.*, Z. Physik **A279**, 399 (1976).
[11] H. Genzel *et al.*, Z. Physik **A268**, 43 (1974).
[12] H. Ströher, priv. comm.
[13] G. Barbiellini *et al.*, Phys. Rev. **174**, 1665 (1968).
[14] P. Dougan *et al.*, Z. Physik **A276**, 155 (1976).
[15] V.B. Ganenko *et al.*, Sov. J. Nucl. Phys. **23**, 162 (1976).
[16] R.L. Workman and R.A. Arndt, solution FA93, *Scattering Analysis Interactive Dial-in* (SAID) program, available by TELNET to VTINTE (*physics;quantum*). The FA93 and SM95 solutions are essentially identical at these energies.
[17] A. I. L'vov, Sov. J. Nucl. Phys. **34**, 597 (1981); and priv. comm.
[18] A.M. Sandorfi *et al.*, *Topical Workshop on Excited Baryons-1988, Troy NY* (ed. by G. Adams, N. Mukhopadhyay and P. Stoler), World Scientific, Singapore, 256 (1989).

Two-Nucleon Knockout from ^{16}O with Polarized Photons (Exp. L17)

R. Lindgren[5], H. Baghaei[5], A. Caracappa[1], A. Cichocki[5], G. Davenport[2], R. Finlay[2], V. Gladyshev[5], T. Gresko[5], K. Hicks[2], S. Hoblit[1], M. Khandaker[6], O. Kistner[1], A. Kuczewski[1], F.X. Lee[4], M. Lucas[3], L. Miceli[1], B. Norum[5], J. Rapaport[2], A. Sandorfi[1], R. Sealock[5], L.C. Smith[5], C. Thorn[1], S. Thornton[5], C.S. Whisnant[3], and L.E. Wright[2]

[1]Physics Department, Brookhaven National Laboratory, Upton N.Y.,11973;
[2]Department of Physics, Ohio University, Athens, OH 45701
[3]Department of Physics, University of South Carolina, Columbia S.C.,29208;
[4]TRIUMF, 4004 Wesbrook Mall, Vancouver, B.C., V6T 2A3, Canada;
[5]Department of Physics, University of Virginia, Charlottesville Va.,22903;
[6]Physics Department, Virginia Polytechnic Institute & SU, Blacksburg Va.,24061.

Cross sections and asymmetries have been measured for the photo-nuclear reactions ^{16}O(γ,pn) and ^{16}O(γ,pp) by bombarding a 10 cm long water target with linearly polarized tagged photons with energies in the range from 205 to 315 MeV. Measurements have been made for the first time in broad kinematics with linearly polarized photons to make detailed comparisons of asymmetries and cross sections with model calculations. By using the data to constrain elements of the nuclear models, we hope to obtain

better understanding of the two nucleon knockout reaction process, associated two body currents, short range nuclear correlations, and higher order multi-nucleon absorption effects.

The detector system used for the experiment included an upper array of 32 plastic scintillation bars, 10 x 10 x 160 cm^3 in 2 layers of 16, and preceeded by another 16 thin paddles, 11 x 1 x 160 cm^3. This array covered an angular range from 20 to 140 degrees with respect to the photon beam and was used to identify protons and neutrons. The p/n energy was determined by time-of-flight from the target, and the position along the bar was determined from mean timing. A second array beneath the target consisted of CsI and plastic scintillation blocks covering an angular range of 25 to 165 degrees with scintillation paddles forming a ΔE- E telescope to identify and measure the energy of the stopped protons. To facilitate calibrations and normalizations, cross sections and asymmetries for $^2H(\gamma,pn)$ were also measured using a heavy-water target.

Cross sections and asymmetries have been extracted in coplanar and symmetrical kinematics for various missing energies for pn and pp events at 220, 260 and 300 MeV incident beam energy. For these kinematics both nucleons have the same energy and are detected at equal angles on opposite sides of the beam line. For 300 ±15 MeV incident photons, cross sections for pn and pp are shown in the upper panel of figure 1 and asymmetries in the lower panel. With the additional constraint on the missing energy of 25 ±15 MeV, the energy of the detected protons and neutrons is 138 ±15 MeV, corresponding to the removal of two nucleons from the p shell in ^{16}O. There are three striking features exhibited by the data. One is the peak in the angular distribution centered at about 75 degrees in both pn and pp. This is the expected position for two-body absorption with subsequent emission of equal momentum proton and neutron on opposite sides of the beam line (– the *quasi-deuteron* regime). The second is the fast fall-off of the cross section with proton angle on either side of the peak. Another feature characteristic of this data is the uniformly negative asymmetry in the range from -0.1 to -0.3 at angles where the cross section

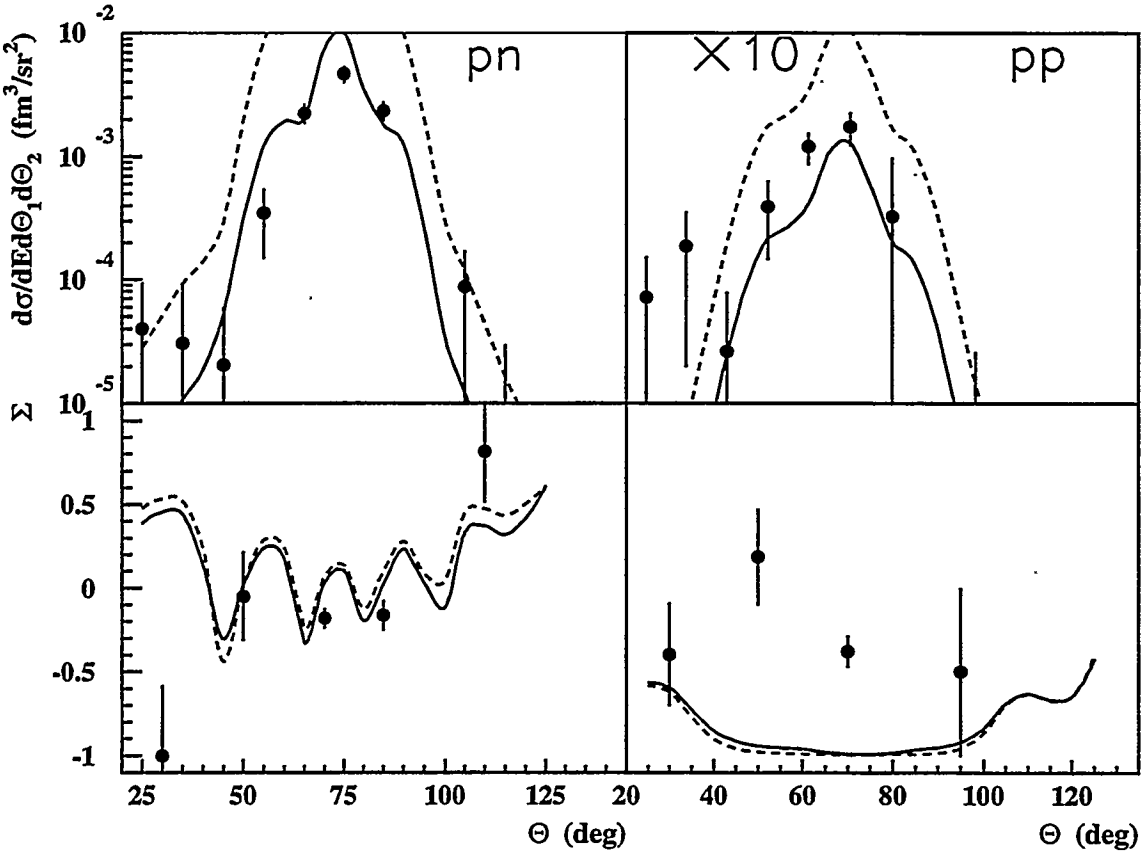

Fig. 1. The upper left and right panels show the $^{16}O(\gamma,pn)$ and $^{16}O(\gamma,pp)$ cross sections, respectively, for 300 ± 15 Mev photons. Here, the emitted nucleons are detected in a symmetrical coplanar geometry with $E_p=E_n=138 \pm 15$ MeV and $\Delta E_m=25 \pm 15$ MeV. The lower panels show the corresponding polarization asymmetries, $\Sigma = (\sigma_{\parallel} - \sigma_{\perp}) / (\sigma_{\parallel} + \sigma_{\perp})$.

is near maximum. These three features are characteristic of most of the pn and pp data taken in coplanar symmetrical kinematics for 220 to 300 MeV incident photons and missing energies up to 80 MeV.

Calculations of photon absorption by a pair of nucleons in ^{16}O, including one body and two body currents in the framework of a shell model, have been done by thegroups at Pavia [1] and Ghent [2]. Recent results calculated by the Pavia group [3] are shown in figure 1. The one body current includes the effects of a Jastrow type correlation function and the two-body current includes diagrams corresponding to the delta isobar current. The seagull meson-exchange current distortion effects are included by optical model calculations. For the curves shown in figure 1 a hypernetted chain model [4] is used to calculate the correlation function and two different models are used to calculate the isobar current, which is the dominant term in the calculation of the cross section for both pn and pp. The full line in the figure refers to the calculation that models the isobar current using a static propagator. The shape of the cross section angular distribution is nicely predicted by the calculation for both pn and pp. Similar fits have been obtained for the 220 and 260 MeV photon data. Previous theoretical treatments [5] have shown that the shape is essentially modulated by a function which is the probability of finding the total momentum of the pair in some initial state P. (The shape will not be sensitive to the explicit absorption mechanism.)

On the other hand, the magnitude of the cross sections depends on many factors including the details of the absorption models and how the continuum of final states is treated. In the Pavia model, the total strength is assumed to come from two p shell holes centered at a missing energy of 30 MeV. Clearly, this is a crude approximation. To approximate the spreading of this strength we have summed the data from 10 to 40 MeV missing energy. Again, comparison of the magnitude of the cross sections between the Pavia model and the data is reasonable. The magnitude also depends on the model chosen for the isobar current, the correlation function, initial and final state nuclear wave functions, and the optical model

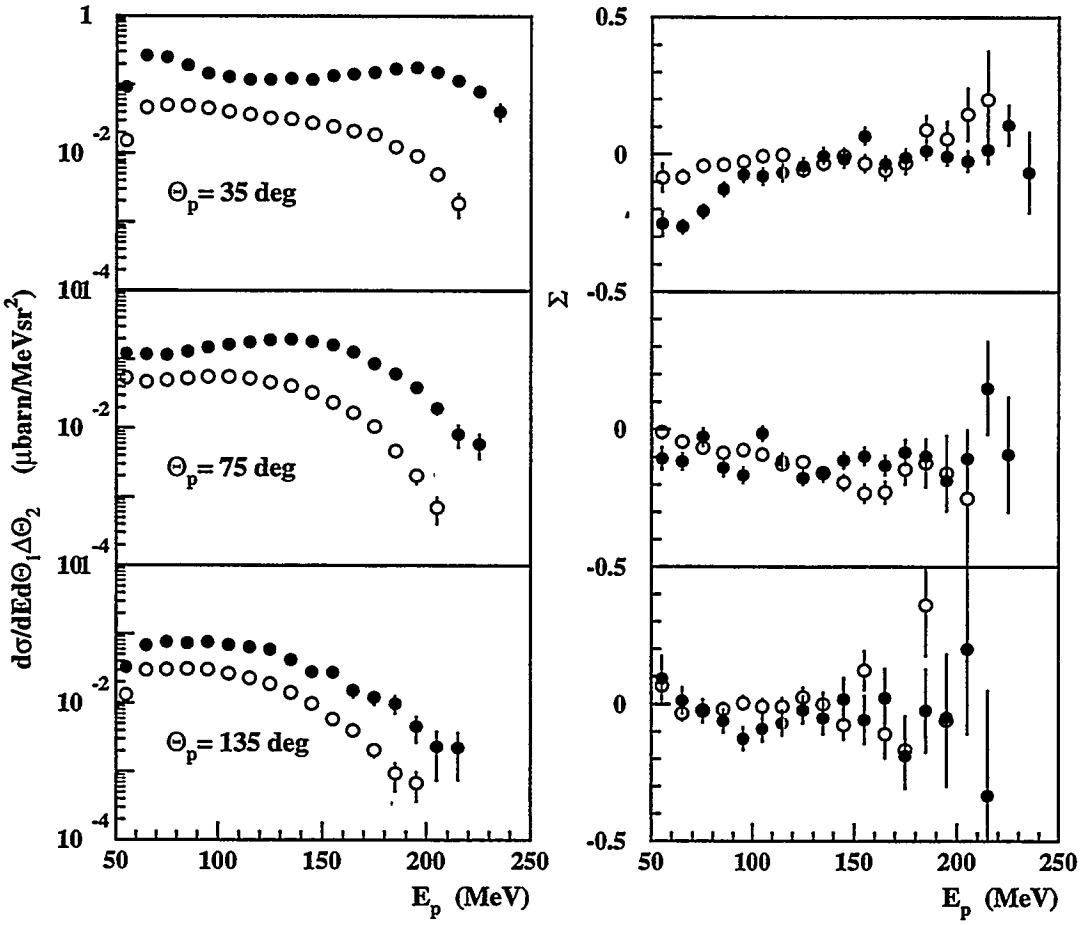

Fig.2. Cross sections and asymmetries for $^{16}O(\gamma,pn)$ and $^{16}O(\gamma,pp)$ at 300 MeV are plotted as filled and open circles, respectively, against the energy of a detected proton. The energy and angle of the other nucleon has been summed over.

used to calculate the distortions. The calculations shown by the dotted line in figure 1 use a similar expression for the isobar current, but with an energy dependent propagator and a factor representing the Δ decay width. This gives a worse fit to both sets of data but illustrates some of the sensitivities.

The asymmetry is considerably less sensitive to scaling factors that could effect the one body and two body currents, while being more sensitive than the cross section to the smaller amplitudes through interference effects. The comparison to the pn data in the bottom panel of figure 1 is not bad, but the comparison to the pp data is quite poor. A different correlation model, not shown here, derived from the OMY potential predicts positive asymmetries [1] for the pn data, which illustrates the sensitivity of this polarization observable. In the calculation shown in figure 1, the asymmetry for pn appears to result from an interference between the isobar current and the seagull diagram in meson exchange, since it is not present in the pp calculations. Similar pn and pp absorption calculations in a shell model framework have been performed by the Ghent group [2]. The magnitude of the cross sections approximately fit the data and the asymmetry for the pp data is in closer agreement than the results shown here.

In figure 2, the pn and pp cross sections and asymmetries at 300 ± 15 MeV are shown. Here, the angle and energy is summed over one of the nucleons, and the cross section is plotted as a function of the energy of the other proton at specific proton angles. The filled circles correspond to the pn data where the neutron is summed over and the open circles correspond to pp data where the proton is summed over. The ratio of the pn to pp cross section is not constant, but varies from 30/1 at 200 MeV proton energy and forward angles to 3/1 at 60 MeV and backward angles.

Further analysis of the data is in progress, emphasizing other kinematics, and additional theoretical work is required in order to disentangle the important components of the reaction mechanisms.

[1] S. Boffi, C. Giusti, F. D. Pacati and M. Radici, Nucl. Phys. **A564**, 473 (1993);
C. Giusti, F.D Pacati and M. Radici, Nucl. Phys. **A546**, 607 (1992).

[2] J. Ryckebusch, Proceedings of the Second Workshop on Electromagnetically Induced Two-Nucleon Knockout, Ghent, Belgium May 1995

[3] C. Giusti, private communication

[4] G. Co' *et al.*, Nucl. Phys., **A549**, 439 (1992)

[5] J. Ryckebusch, M. Vanderhaeghen, L. Machenil, and M. Waroquier, Nucl. Phys. **A568** (1994),

Polarized Photon scattering from ^{4}He (Exp. L16)

V- Bellini[1-2], M. Capogni[3], A. Caracappa[4], L. Casano[3], A. D'Angelo[3], F. Ghio[7], B. Girolanii[7], S. Hoblit[4,8], L.Hu[3], M. Khandaker[4,9], O.C. Kistner[4], A.I. L'vov[11], L. Miceli[4], D. Moricciani[3], V.A. Petrun'kin[11], A.M. Sandorfi[4], C. Schaerf[3,13], and C.E. Thorn,

[1]Physics Department, University of Catania, Corso Italia 57, 1-95129, Catania, Italy
[2]INFN-LNS, Via S. Sofia II, 1-95125, Catania, Italy
[3]INFN-Itoma 2, Via delta Ricerca Scientiflca I, 1-00133, Rome, Italy
[4]Physics Department,Brookhaven National Laboratory, Upton N. Y. 11973, USA
[7]Istituto Superiore di Sanit£ and INFN-ISS, Viale Regina Elena 299, 1-00161, Rome, Italy
[8]Physics Department, University of. Virginia, Charlottesville, VA 22.901
[9]Physics Department, Virginia Polytechnic Institute & State University, Blacksburg, VA 2$061
[11]Lebedev Physical Institute,Lenizzsky Prospect 53, 11792$, Moscow, Russia
[13]physics Department, University of Rome "Tor Vergata", Via della Ricerca Scientiflca I, 1-00133, Rome, Italy

Although the Δ-hole model has been relatively successful in accounting for a large body of π-N scattering data, it has failed to reproduce recent measurements of scattering with unpolarized photons [1], particularly at energies below the Δ peak. In contrast, calculations of quasi-free scattering have succeeded in reproducing the main features of these data [2]. A number of different dynamical effects are modeled in these calculations and polarization observables, which can often be sensitive to interference terms that are masked in the spin average cross sections, can potentially provide an important constraint.

In this experiment, Compton scattered photons were detected in a large high-resolution NaI spectrometer. Compton separation was enhance by another NaI array surrounding the target which vetoed π^o-decays. Data for the two linear polarization states are shown at 224 and 310 MeV in figure 1.

The solid curves in the figure are the full predictions of the updated model of Ref [2]. This model

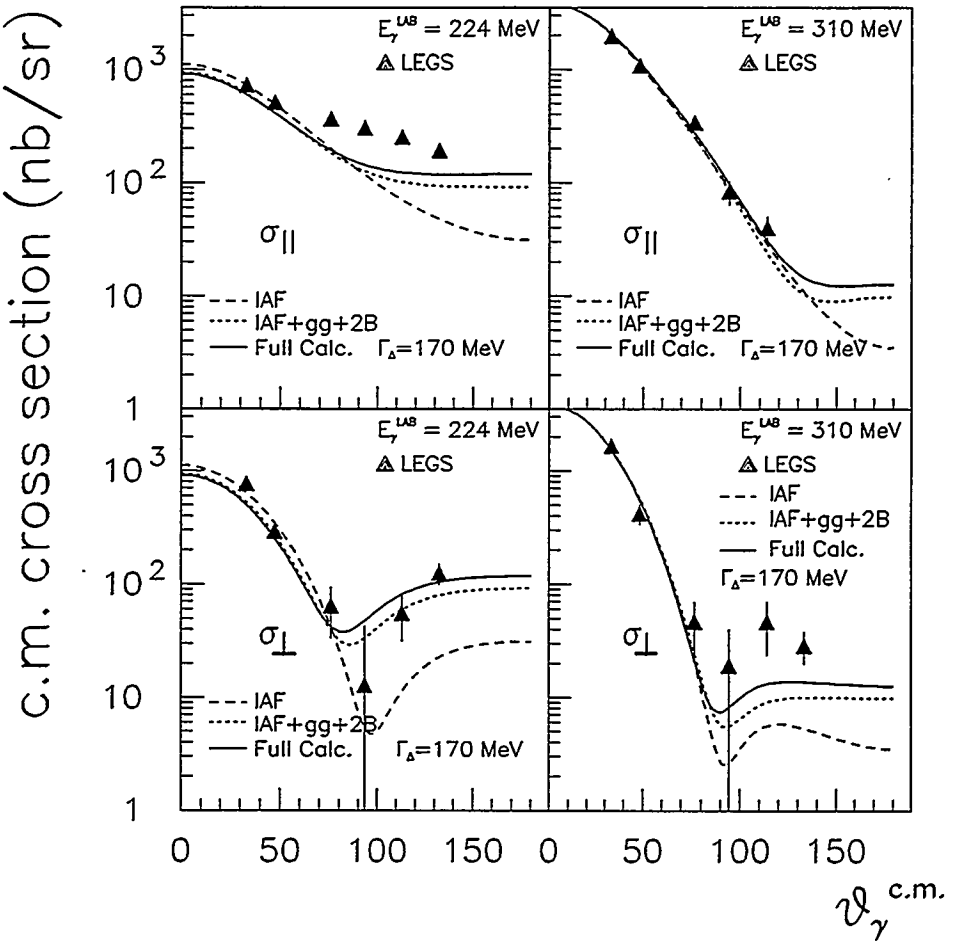

Fig. 1. Compton cross sections for scattering from ^{4}He at 224 MeV (left panels) and 310 MeV (right panels), with incident photon polarization parallel (top) and perpendicular (bottom) to the scattering plane.

utilizes through an impulse approximation γ-nucleon scattering amplitudes known from relativistic dispersion relations [2j. In the present version the γN-amplitude was calculated with the VPI(SM95) (γ,π) multipoles taken as input. Medium and off-shell modifications of the γ-N amplitude were introduced (i) through Fermi smearing of the incoming photon energy (dashed *IAF* curves), (ii) through off-shell corrections to vertices of the subprocess γN →Δ→ γN which dominates γN-scattering at these energies, and (iii) through increase of the intermediate-Δ width to 170 MeV. Such an enlarged width is required to reproduce the magnitude, and general shape of the total photoabsorption cross section of ^{4}He(γ,X) which is related through the optical theorem to the γ-N amplitude. This effective width takes into account the bulk of MI mesonic exchange currents. Additional smaller modifications of the Δ are provided by diagrams with exchanged π (or ρ) and direct photon coupling to the πNΔ vertex [2].

Electric EI mesonic-exchange effects are also important. They result in a strong enhancement of cross sections at backward angles (dotted curves). These effects were approximately taken into account through a Siegert-like procedure of minimal substitutions applied to effective momentum-dependent nucleon nucleus vertices.

The model reproduces the general trends in the data. With the enlarged width of the Δ a satisfactory agreement is found at all energies at forward angles. However, the model underestimates $d\sigma_{||}$ at central angles and low energies and $d\sigma_\perp$ at high momentum transfer. A more direct evaluation of the contribution of meson-exchange currents is probably needed to explain the remaining discrepancy.

[1] E.J. Austin *et al.*, Phys. Rev. Lett. **57**, 972 (1986); E.J. Austin *et al.*, Phys. Rev. Lett. **61**, 1922 (1988); D. Delli Carpini *et al.*, Phys. Rev. **C43**, 1525 (1991).
[2] A. L'vov and V. Petrun'kin, Lecture Notes in Phys. **365**, 123 (1990).

The signature of diprotons in $^3He(\vec{\gamma},pp)n$

A.M. Sandorfi[1] and W. Leidemann[2]

[1]Physics Department, Brookhaven National Laboratory, Upton NY 11973
[2] Dipartimento di Fisica, Università di Trento, I-38050 Povo (Trento)

Although the internal structure of the nucleon guarantees the existence of three-body components to the nuclear force, definitive signatures of three-body effects have remained rather elusive. In recent efforts to isolate processes involving three nucleons, considerable activity has focused on the ^{3}He(γ,pp)n reaction at intermediate energies [1-4]. For the most part, the motivation for these experiments has been the observation by Laget [5] that for kinematics in which the neutron has low momentum, 2N components which usually overwhelm the 3N currents should be dramatically suppressed. (This is to be expected since an S=0 diproton has no dipole moment and charged π-exchange cannot contribute.) For such cases, deviations from complete calculations using only two-body potentials might reveal three-body force effects.

Arguments for an enhancement of 3N currents in ^{3}He(γ,pp)n have rested on the absolute magnitudes of cross sections as compared to Laget's predictions using a diagrammatic expansion of static two-body interactions [1-4], and on comparisons with recent polarization asymmetry measurements at LEGS [3].

Recently, the TAGX Collaboration [4] have taken a further step by proposing a decomposition of missing-neutron momentum distributions from ^{3}He(γ,pp)n into distinct 2N and 3N components. While they associate the dominant contribution with 3N absorption mechanisms, they have argued that the smaller and lower-momentum 2N part suffers little contamination from FSI, and so essentially represents the photodisintegration of $^1S_0$ diprotons.

We have examined the polarization asymmetry that would result from the photodisintegration of an $^1S_0$ diproton in ^{3}He. The results are dramatically different from quasi-deuteron breakup and can aid in the interpretation of ^{3}He(γ,pp)n experiments.

Because of the symmetry between the identical particles of a *p-p* pair, $M(J_{odd})$ transitions are not allowed, $E(J_{even})$ transitions can only occur with channels spin zero, and $M(J_{even})$ or $E(J_{odd})$ transitions can only only occur for channel spin one. As a result of these symmetry restrictions, interfering multipoles of opposite parity *all* vanish, and angular distributions of both cross sections and polarization asymmetries contain only even powers of $\cos(\theta)$ [6,7]. Furthermore, cross sections measured with the photon's electric vector parallel to the reaction plane are always directly proportional to powers of $\cos^2(\theta)$ and vanish at 90°. This forces the polarization asymmetry to take the extreme value of –1 at 90° c.m.

These symmetry considerations are all referred to the diproton-photon center of momentum (c.m.). These will be altered by the motion of the *p-p* pair relative to the ^{3}He nucleus. This effect is naturally incorporated in realistic ^{3}He wavefunctions obtained from solutions of the three-body Faddeev equations. The diproton wavefunction then depends upon the single particle (neutron) momentum, q, corresponding to a momentum for the *p-p* pair of 2/3 q relative to the ^{3}He c.m. This calculation has been performed for a dominant $^1S_0$ diproton and s-wave neutron initial state. The wavefunction was taken from a 34 channel Faddeev solution of the Bochum group for the three-nucleon system with the Paris potential [8]. The pair wavefunction was calculated from the Faddeev components applying the proper antisymmetrization [8]. The resulting $^1S_0$ pair with the third particle in a relative s-wave accounts for 44.5% of the total normalization. For comparison, the $^3S_1$(np) pair contributes 44.9%, and the $^3D_1$(np) pair 2.9%, with the third particle again in a relative s-wave. The remaining 7.7% is spread over all the other configurations. Neglecting the interaction of the final *pp* pair with the s-wave neutron reduces the full three-body problem to the interaction of two outgoing nucleons. However, the important Δ degrees of freedom are explicitly included in the electromagnetic and strong interactions. For the latter we have solve coupled channel equations with nucleons and deltas, using the Argonne V28 potential.

For diprotons in ^{3}He, the LAB angle that corresponds to 90° in the *p-p* c.m. will depend upon the Fermi momentum of the pair. The transformed LAB asymmetry, weighted by the *p-p* pair momentum

distribution, is shown as the solid curve in figure 1 [7]. Although the predicted asymmetry never reaches –1, it remains very large and negative over a broad angular range.

In contrast, the measured beam asymmetry (solid circles in fig. 1) is quite small at all proton angles and does not support the identification of the low missing-neutron momentum component with simple $^1S_0$ diproton breakup. That being the case, it is quite unlikely that the neutron momentum distribution can be simply decomposed as an incoherent sum of "2N"+"3N" components, as proposed in ref. [4].

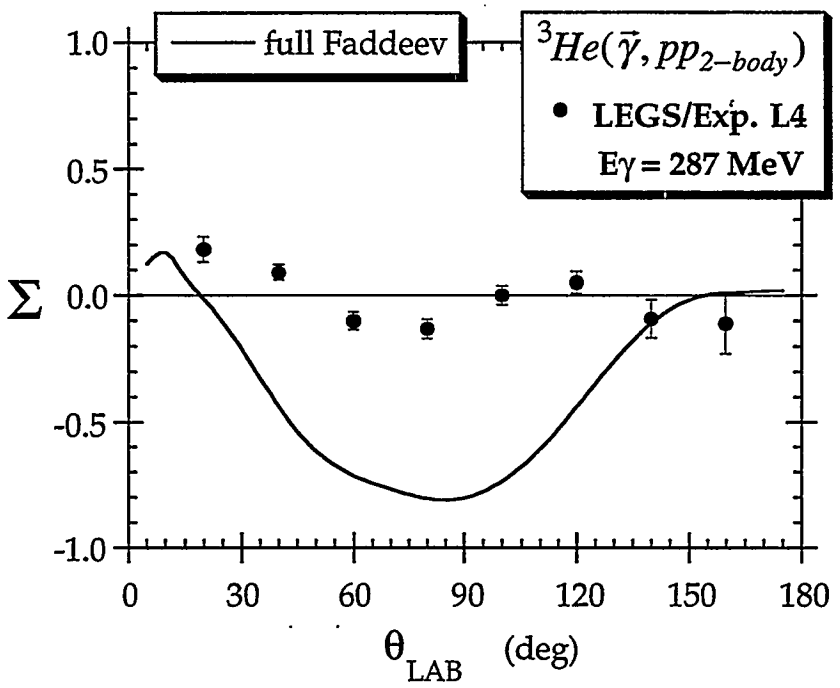

Fig. 1. The curve gives the expected asymmetry for the photodisintegration of a diproton in ^3He from the calculation of ref. [7], transformed to the LAB and weighted by the *p-p* pair momentum distribution. The solid points are the measured ^{3}He(γ,pp)n values [3,7], integrated over the momenta that would correspond to *p-p* breakup.

[1] A. Sarty *et al.*, Phys. Rev. **C47**, 459 (1993).
[2] G. Audit *et al.*, Phys. Lett. **B312**, 57 (1993).
[3] D.J. Tedeschi, *et al.*, Phys. Rev. Lett. **73**, 408 (1994).
[4] T. Emura *et al.*, Phys. Rev. Lett. **73**, 404 (1994).
[5] J.-M. Laget, J. Phys. **G14**, 1445 (1988); Nucl. Phys. **A497**, 391c (1989).
[6] A.M. Sandorfi, *Few Body Physics with Polarized Photons*, Int. Sym. High Energy Spin Physics and Polarization Phenomina in Nuclear Physics, Bloomington, Indiana, 1994, ed. E.J. Stephenson and S. Vigdor, AIP**339** (1995).
[7] A.M. Sandorfi and W. Leidemann, Phys. Rev. C**53**, 1506 (1996).
[8] H. Kamada, private communication; W. Glöckle, *The Quantum Mechanical Few-Body problem*, Springer-Verlag, Berlin-Heidelberg (1983); D. Hüber, H. Kamada, H. Witala, and W. Glöckle, Few-Body Syst. **16**, 165 (1994).

Nucleon Spin Structure – Preparations for Double Polarization Experiments:

A variety of sum rules have been derived that can potentially be used to study the spin structure of the nucleon. These use integrals of photo-reaction cross sections sections measured with photon and nucleon spins parallel, $\sigma_{3/2}$, and anti-parallel, $\sigma_{1/2}$.

Two that are particularly sensitive are the Spin-dependent Polarizability (γ), and the Drell-Hearn-Gerasimov (DHG) integrals. Both of these arrise from considerations of the forward Compton scattering amplitude [1]. γ can be calculated with chiral perturbation theory and obeys a sum rule, weighted by the third power of photon energy, running from π-threshold (ω_0) to infinity.

$$\gamma = \frac{1}{4\pi^2} \int_{\omega_0}^{\infty} \frac{\sigma_{1/2} - \sigma_{3/2}}{\omega^3} \, d\omega$$

A Gell-Mann/Goldberger/Thirring dispersion relation relates the same difference of spin-dependent cross sections, but now weighted by a single power of the energy, to the anomalous magnetic moment (κ) of the target and to the spin-flip forward Compton amplitude at infinity, g(∞). As first suggested by Drell, Hearn and Gerasimov, g(∞) is usually assumed to be identically zero.

$$DHG = \int_{\omega_0}^{\infty} \frac{\sigma_{1/2} - \sigma_{3/2}}{\omega} \, d\omega = -\frac{2\pi^2 \alpha}{m^2} \kappa^2 - 4\pi^2 \, g(\infty)$$

As yet there are no direct measurements of $\sigma_{1/2}$ or $\sigma_{3/2}$, but extrapolations of single-polarization data using (model-dependent) multipole analyses lead to a serious inconsistency between the standard model predictions for these sum rules for the proton-neutron difference [1].

Experiments will begin at LEGS in 1997 to measure the $\sigma_{3/2}$ and $\sigma_{1/2}$ double-polarization cross sections from threshold to 470 MeV.

[1] A.M. Sandorfi, C.S. Whisnant and M. Khandaker, Phys. Rev. **D50**, R6681 (1994).

Instrumentation Development:

The LEGS-Spin Collaboration:

Brookhaven Nat. Lab., Laboratori Nat. di Frascati-INFN, Univ. Gießen, Norfolk State, Ohio Univ., IPN Orsay, Univ. Roma II, Univ. South Carolina, Syracuse Univ., Virginia Polytech, Univ. Virginia

The future LEGS experimental program is dependent upon (i) a new **S**trongly **P**olarized **H**ydrogen-deuterium **ICE** (SPHICE) target of frozen hydrogen-deuteride (HD) in which both nuclear species can be independently polarized, and (ii) a new large acceptance **S**pin-**ASY**mmetry (SASY) detector for both neutrals (γ, n, π^0) and charged particles (p, π^+, π^-). There has been considerable progress on both.

The **S**trongly **P**olarized **H**ydrogen-deuteride **ICE** (**SPHICE**) target

The LEGS Spin Collaboration is developing a solid Hydrogen-Deuteride target (SPHICE) for photonuclear experiments. A short spin-lattice relaxation time is required to polarize this target in a reasonable time by the brute force method of high magnetic field and low temperature. On the other hand, a long relaxation time is required to "freeze" the polarization during transport, storage and the running of nuclear physics experiments. These seemingly opposing requirements are met by exploiting the dependence of the relaxation time of the H and D nuclei in the HD target on the concentrations of the metastable J=I molecular species of H_2 and D_2 impurities. Including an appropriate doping of the HD target material with a small amount of J=I H_2 leads to an initially short H-relaxation time which then lengthens as the J=I H_2 decays exponentially to the J=0 state with a 6.5 day time-constant. Although the analogous procedure can be used to polarize the deuterium, the longer decay time for J=I D_2 (18.2 d) makes it more practical to transfer H polarization to the D with an rf transition and then repolarize the H.

Development work on this new target started in 1993. Since then, there has been considerable progress, and two Technical Reviews of the project. Proton spin relaxation times of 30 days at 1.0 T and 0.45 °K were observed in January 1995. In the summer of 1995, two critical experiments were successfully completed. The first concerns the ability to remove heat from the HD during the low temperature polarization phase. The second is the demonstrated ability to retrieve a polarized target into a warmer (4 - 5 °K), lower field (0.045 - 0.15 T) environment while maintaining the polarization.

As the *ortho*-H_2 impurity decays to its *para*-state, heat is generated within the target which , if not conducted away, would raise the HD temperature and thereby reduce the attainable equilibrium polarization. In the SPHICE targets this temperature rise is limited by high thermal conductance metal cooling wires. Although this entails a cost in dilution of the polarized H and D nuclei with other unpolarized nudeons , the results of experiments with small (0.25 cm^3) HD samples have demonstrated that the required low temperatures and high polarizations can be achieved with aluminum cooling wires constituting only 5% of the target by weight. The main objective of the summer '95 experiments was to verify that the lowest target temperature, and hence the maximum achievable polarization, can be maintained as the target size is scaled up from the 0.25 cm^3 of the previous measurement to the 20 cm^3 of the LEGS targets, using the same target heat generation rate and the same 5% by weight cooling wires. All other effects pertinent to the achievable polarization, such as relaxation time reduction or surface depolarization by paramagnetic impurities, are the same or better for larger targets.

A successful demonstration of the ability to conduct away the decay heat was made in July'95 on a 2 cm^3 sample , ten times the volume of previous test cells and only a factor of two smaller in linear dimensions than the final size targets. A comparison of the temperature of the refrigerator cold finger with that of the sample (as determined by NMR techniques) is shown in figure 1 for both the large and small targets. Both targets have similar areal densities of 1 mil wires and are doped to comparable *ortho*-hydrogen concentrations. The deviation from equal temperatures below ~50 mK, is an indication of the Kapitza (heat flow) resistance at the interface between the wires and the HD. By keeping the areal density of wires the same for the two targets, the base temperature is the same *even though the targets differ by an order of magnitude in volume*. At the end of a polarization cycle, the observed cooling capability in the 2 cm^3 cell would have resulted in H polarizations of 63% under the conditions in the dilution refrigerator (DF) used for this study at Syracuse University, and 80% in the new BNL DF. This is the same level of polarization projected from the previous small sample studies and no problems are expected in scaling up the rest of the way to the full size target. Measured rf-transition efficiencies have demonstrated that D polarizations in excess of 50% will also be achieved under these conditions.

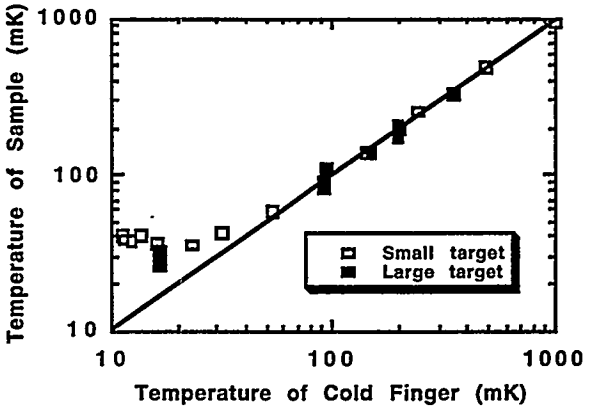

Fig. 1. Comparison of the temperature of the cold finger with that of the sample for large (0.1 mole) and small (0.014 mole) HD targets.

The use of the HD frozen spin target system requires cold transfers among the HD injection cryostat used to initialy freeze the HD, the dilution refrigerator where polarization takes place, the storage cryostat, and finally the in-beam cryostat. In these transfers the target moves through very different magnetic field configurations and regions of varying temperature. A second crucial step toward a usable target is the demonstration that these manipulations can indeed be carried out without polarization loss. The most critical stages, HD injection, polarization in the DF, and extraction from the DF with subsequent verification that the polarization had been maintained, were successfully demonstrated in August'95 using the smaller Syracuse DF facility.

The *still* for production of the large quantities of high purity HD was assembled and tested in January of this year. The Large dilution refrigerator (Oxford-1000) and high field magnet (17 T) for target production, built by Oxford Instruments, has met all specifications and was delivered to Syracuse in April 1996. The first large volume HD targets are expected by the end of this year. The in-beam dewar

is in production at Orsay and will be delivered early in 1997, and the experimental nuclear physics program will start shortly thereafter.

The Spin **ASY**mmetry (**SASY**) array

SASY is a high efficiency, large solid angle detector array providing complete determination of angle, energy, and particle identity for all reactions induced by photons on hydrogen and deuterium. The complete detector package will consist of a central Time Projection Chamber (TPC) for tracking charged particles, surrounded by a layered calorimeter for neutrals. The calorimeter is being constructed first and is nearly complete. The major components are shown in the photo (figure 3) and in the accompaning schematic drawing below (figure 4). An 432 component array of 6.4 cm x 6.4 cm x 30.5 cm NaI(Tl) crystals provides coverage for photons and charged particles in the angular region from 45 to 135 degrees. Forward angles (35 to 7 degrees) are covered by a 96 element wall of plastic scintillators, with a total thickness of 31 cm, and a 176 element array of 15.3 cm x 15.3 cm x 25.4 cm Pb-glass Cerenkov counters. The plastic wall provides charged particle detection and calorimetry as well as a 30% efficiency for the detection of neutrons. (Recoil neutrons from single-pion production are concentrated in forward angles.) The Pb-glass Cerenkov counters provide detection of photons in the forward direction. Together with the NaI array, these systems provide ~80% coverage of 4π. A 0° gas Cerenkov counter (not shown in the figures) will provide on-line rejection of atomic events.

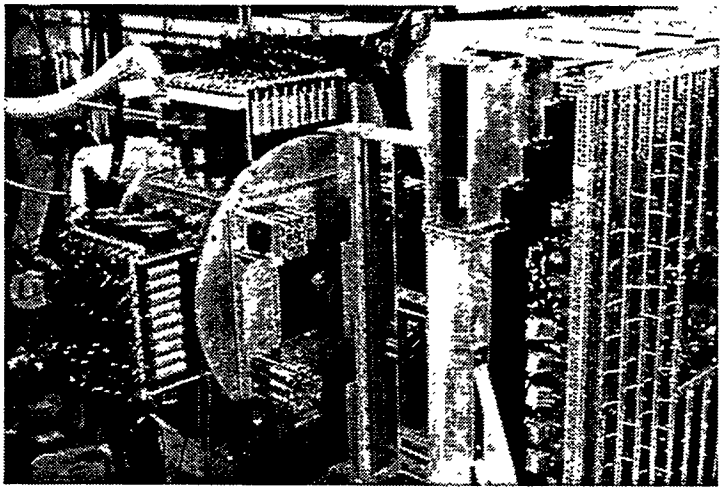

Fig.3. The SASY calorimeter in May, 1996.

The SASY calorimeter package is presently being commissioned in a $D(\gamma,\gamma n)$ measurement of the polarizabilities of the neutron. With minor additions, it will be used in 1997 together with the first SPHICE targets for an initial round of sum rule measurements on the proton. These experiments will simply require the separation of nuclear and atomic events. Measurements on the neutron require the identification of final states. For this a central tracking system is being designed to (1) measure high energy pions in the forward direction, (2) lower the threshold for charged particles in the central region, and (3) provide the sign determination for charged pions. This system will utilize the 1.5 -to- 2.0 T field of a superconducting solenoid (which also provides the holding field for the polarized target), a cylindrical TPC and two forward planar drift chambers. Construction of these tracking components is expected to begin in 1997.

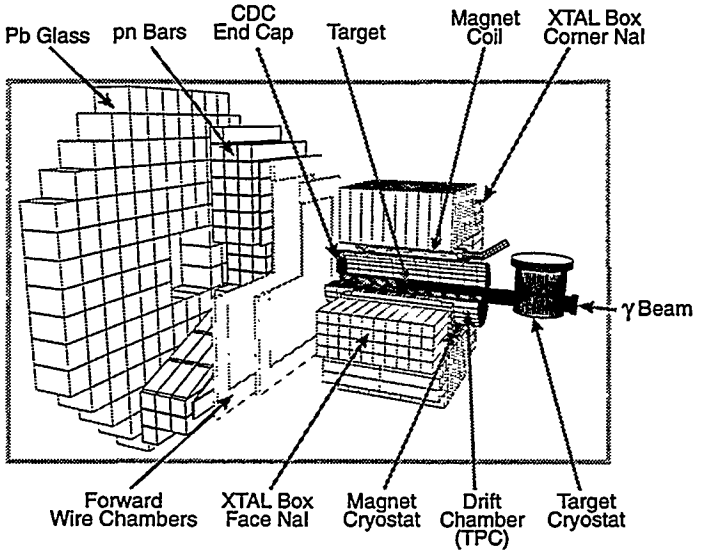

Fig.4. Schematic layout of SASY with the SPHICE target.